*energies*

MDPI

*Article*

# Hydrocarbon Accumulation Stages in the Huhehu Sag, Hailar Basin, China

**Junping Cui [1,2,3], Wei Jin [4], Zhanli Ren [1], Haoyu Song [1], Guoqing Liu [1] and Hua Tao [1,*]**

[1] Department of Geology, Northwest University, Xi'an 710069, China; cuijp@nwu.edu.cn (J.C.); renzhanl@nwu.edu.cn (Z.R.); s200103025015@163.com (H.S.); liuguoqing20210226@163.com (G.L.)
[2] State Key Laboratory of Continental Dynamics, Northwest University, Xi'an 710069, China
[3] National & Local Joint Engineering Research Center for Carbon Capture and Sequestration Technology, Xi'an 710069, China
[4] Exploration and Development Research Institute, Daqing Oilfield, China National Petroleum Corporation, Daqing 163712, China; jinweigeo@pelrochina.com.cn
* Correspondence: thua@stumail.nwu.edu.cn

## Abstract

Huhehu Sag is a sag with high exploration degree in Hailar Basin. With large sedimentary thickness, complete stratigraphic development and excellent oil generation conditions, it is the main oil- and gas-producing sag in Hailar Basin. The primary source rocks are the Nantun Formation, with the Tongbomiao and Damoguaihe Formations as secondary sources. Hydrocarbon accumulation periods in the sag were comprehensively analyzed using methodologies including source rock hydrocarbon generation-expulsion history, authigenic illite dating of reservoirs, and fluid inclusion homogenization temperature analysis. Results reveal two major accumulation stages: Stage 1 (125–90 Ma), corresponding to the depositional period of the Yimin Formation, represented the peak paleo-geothermal regime and the primary hydrocarbon accumulation phase. Intensive hydrocarbon generation and expulsion, coupled with robust migration dynamics, facilitated large-scale oil and gas pooling. Stage 2(65 Ma-now), from the deposition of Qingyuangang Formation to the present, uplift and denudation reduce the burial depth of source rocks, the hydrocarbon generation intensity is weakened. This phase involved secondary adjustments of pre-existing reservoirs and continued charging of newly generated hydrocarbons. The Huhehu Sag is a typical half-graben structure. Fault-block and fault-lithologic reservoirs dominate, distributed zonally along gentle and steep slopes. Lithologic reservoirs primarily occur near or within the central hydrocarbon-generating sub-sags. The most favorable hydrocarbon accumulation zones are located in the sub-sag centers and adjacent areas with high-quality reservoirs.

**Keywords:** hydrocarbon generation-expulsion period; illite dating; fluid inclusions; hydrocarbon accumulation stage; hailar basin

check for updates

Academic Editor: Reza Rezaee

Received: 14 July 2025
Revised: 30 September 2025
Accepted: 9 October 2025
Published: 17 October 2025

**Citation:** Cui, J.; Jin, W.; Ren, Z.; Song, H.; Liu, G.; Tao, H. Hydrocarbon Accumulation Stages in the Huhehu Sag, Hailar Basin, China. *Energies* **2025**, *18*, 5488. https://doi.org/10.3390/en18205488

**Copyright:** © 2025 by the authors. Licensee MDPI, Basel, Switzerland. This article is an open access article distributed under the terms and conditions of the Creative Commons Attribution (CC BY) license (https://creativecommons.org/licenses/by/4.0/).

## 1. Introduction

The analysis of hydrocarbon accumulation stages represents a core focus in modern petroleum geology research, as determining these stages helps to deeply understand hydrocarbon reservoir formation patterns. Recent years have seen significant advancements in hydrocarbon accumulation chronology, with the development of various analytical methods, including trap formation period analysis, saturation pressure method, source rock hydrocarbon generation-expulsion history analysis, reservoir authigenic illite dating,

and fluid inclusion homogenization temperature (FIT) analysis. However, these methods differ in their chronological constraints: trap formation analysis and source rock generation-expulsion history determine the earliest possible accumulation time, while the saturation pressure method and authigenic illite dating can constrain the absolute age of accumulation. The FIT method, when combined with basin thermal history and burial history, enables the identification of multi-stage accumulation events [1–8]. There are many methods to restore the thermal evolution history of the basin. At present, the research on the methods of restoring the thermal history of the basin at home and abroad can be generally divided into two categories: one is to restore the thermal history by using various ancient temperature scales, mainly including organic matter maturity index (Ro), fluid inclusions, illite crystallinity index, and apatite and zircon thermal dating methods, and the other is to restore the thermal history by using the thermodynamic model of basin evolution. Because the ancient temperature scale method can check the simulation results through the measured data, it is considered to be a practical method with high research accuracy [9–14]. This study is mainly based on the restoration of burial history, using the EASY%Ro method to simulate thermal history [10]. Although there are many methods to determine the formation period of oil and gas reservoirs, due to varying influencing factors and analytical precision among these methods, integrating multiple approaches comprehensively is critical for accurately determining hydrocarbon accumulation periods.

The Hailar Basin is located in the southwestern part of Hulunbuir League, Inner Mongolia Autonomous Region, bounded by the western shore of Hulun Lake and the Bayanhushu line to the west, extending to the Yimin River to the east. Its northern limit is defined by the Chen Barag Banner, while the southern boundary reaches Buir Lake (straddling the China–Mongolia border), with a small portion extending into Mongolian territory. Geologically, the basin forms part of the Central Asia–Mongolia geosyncline, demarcated by the Derbugan Fault, which separates the Ergun fold system to the west from the Inner Mongolia–Greater Khingan fold system to the east, positioning it at the junction between these two-fold systems. This Meso–Cenozoic faulted basin overlies the Hercynian folded basement [15,16].

As key exploration targets for Daqing Oilfield in recent years, the Wuerxun and Beier sags located in the southern part of the basin have achieved significant hydrocarbon breakthroughs, with current annual production exceeding 500,000 tons. The Huhehu Sag, located in the southeastern Hailar Basin, is a secondary tectonic unit and a half-graben faulted depression.

The Huhehu Sag exhibits excellent hydrocarbon generation conditions, with a total of 18 wells drilled to date. Hydrocarbon shows have been observed in all wells except Haishen-7, Hui-1, He-3, He-4, and He-15. Notably, low-yield oil flows were obtained from He-18 and He-X1 wells, while commercial hydrocarbon flows were achieved in He-10 and He-17 wells, demonstrating significant exploration potential.

While previous studies have investigated the structural characteristics, sequence stratigraphy, depositional systems, organic matter types, hydrocarbon generation potential, reservoir characteristics, and thermal evolution history of the Huhehu Sag [17–25], no comprehensive comparative analysis has been conducted on hydrocarbon accumulation stages, and this gap has constrained the progress of hydrocarbon exploration. This study employs multiple methods including source rock hydrocarbon generation-expulsion history analysis, illite dating, and fluid inclusion thermometry to conduct detailed research on hydrocarbon accumulation stages in the Huhehu Sag and analyze the hydrocarbon accumulation processes and models. The findings hold significant theoretical and practical importance for guiding future exploration activities.

## 2. Regional Geological Setting

The Hailar Basin is a fault-depression basin formed on Hercynian folded basement [15,16], having undergone two major evolutionary stages: rifting and depression [26,27]. During the Jurassic, mantle upwelling transformed the tectonic regime from compressional to extensional, accompanied by extensive volcanic eruptions. The Early Cretaceous marked the peak development stage of the fault-depression basin, witnessing intense extension during Tongbomiao Formation deposition, rapid extension during Nantun Formation deposition, stable extension during Damoguaihe Formation deposition, and overall uplift shrinkage during Yimin Formation deposition. This period was characterized by intense faulting, frequent volcanism, and expanding depositional areas with gradually deepening water bodies forming thick sedimentary sequences in the depression centers. From Late Cretaceous to present, the basin entered a depression stage, experiencing regional compressional uplift across the entire basin. Under the nearly east-west compression, the fault-depressions underwent inversion, depositing fluvial-swamp facies, conglomerates, and mudstones.

The current tectonic framework features two uplifts (Cuogang and Bayanshan) and three depressions (Zalainuoer, Beierhu, and Huhehu), with these first-order tectonic units further subdivided into 16 sags and 4 highs. The Huhehu Sag, a second-order tectonic unit measuring 90–100 km long, 20–40 km wide (covering 2500 km$^2$), is characterized as a half-graben fault depression (Figure 1). Bordered by the Bayanshan Uplift to the west and Xilinbeier High to the east, it extends southward into Mongolian territory, with maximum cover thickness exceeding 4000 m. The stratigraphic sequence comprises, from bottom to top, Jurassic Tamulangou($J_3t$), Cretaceous Tongbomiao ($K_1t$), Nantun ($K_1n$), Damoguaihe ($K_1d$), Yimin ($K_1y$), and Qingyuangang ($K_2q$) formations, followed by Paleogene, Neogene, and Quaternary systems [19,27].

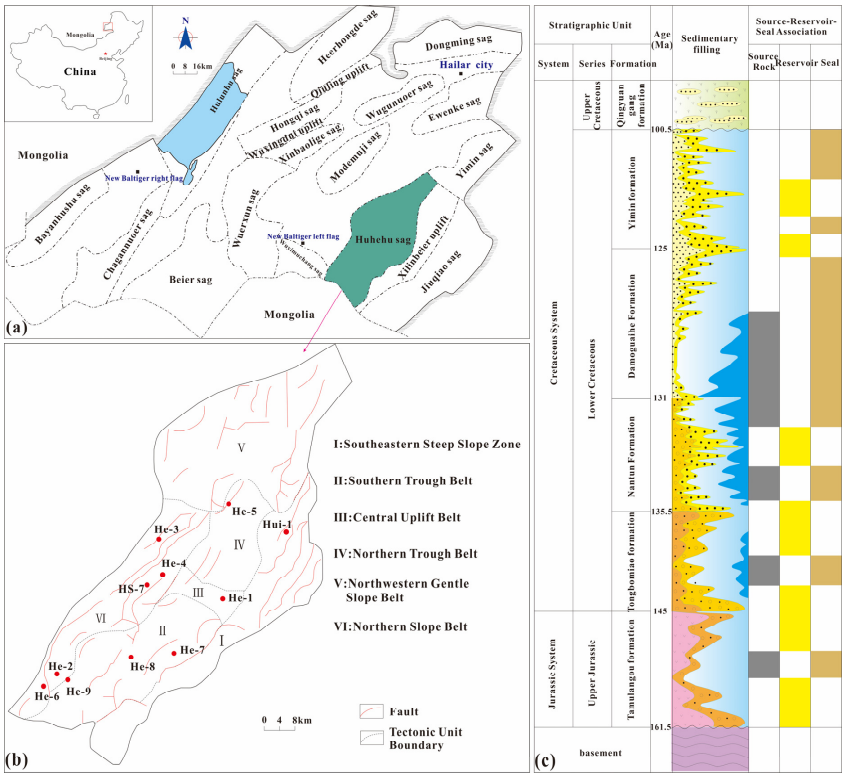



**Figure 1.** The location and drilling distribution map of Huhehu sag. (**a**) Tectonic units of Hailar Basin; (**b**) Tectonic units of Huhehu sag; (**c**) Stratigraphic profile map.

## 3. Materials and Methods

In this work, all of the analyzed rock samples were collected from Huhehu Depression in the Hailar Basin. The sampling principle follows the selection of representative samples. The dating object of authigenic illite dating method is authigenic illite minerals in sandstone reservoirs. Firstly, clay minerals with particle size less than 0.1 μm are separated by separation and purification technology. The mineral composition and sample representativeness were confirmed by scanning electron microscope (Quanta 400, FEI company, Brno, Czech Republic), transmission electron microscope (JEM-F200, JEOL Ltd., Tokyo, Japan), and X-ray diffraction (Xradia 520, Carl Zeiss Company, Pleasanton, CA, USA) [28]. Potassium content is determined by atomic absorption spectroscopy employing an acid dissolution method. During sample fusion at 1500 °C, a precisely measured 38Ar spike is introduced to determine the mixed isotopic ratios ($^{40}Ar/^{38}Ar$ and $^{38}Ar/^{36}Ar$) by isotope mass spectrometry, from which the radiogenic $^{40}Ar$ component is derived. The age is calculated based on the sample's potassium content using the following equation: $t = \ln[(^{40}Ar^*/^{40}K)\lambda/\lambda e + 1]$, where $\lambda = 5.543 \times 10^{-10}a^{-1}$ (total decay constant of $^{40}K$) and $\lambda e = 0.581 \times 10^{-10}a^{-1}$ (branching decay constant for $^{40}K$ to $^{40}Ar$ transformation). The minimum illite age obtained represents either the termination of authigenic illite growth or the earliest/maximum age of hydrocarbon accumulation [29–31]. These analyses were performed by the Key Laboratory of the PetroChina Research Institute of Petroleum Exploration & Development.

The primary hydrocarbon generation and expulsion period in source rocks corresponds to the earliest timing of hydrocarbon reservoir formation. The main oil generation stage is determined through basin modeling, integrating pyrolysis simulation experiments, paleotemperature reconstruction, and source rock burial history analysis [32–34]. The software is PetroMod (2016) developed by Schlumberger, Houston, TX, USA. The experimental apparatus consists of three main components: a GCF-0.25L reactor, an XMT-131 digital temperature controller, and a pyrolysis gas and condensate separation-collection system, the experimental instrument comes from Dalian Automatic Control Equipment Factory in China. Samples and deionized water are loaded into the reactor, which is then sealed and subjected to a pressure test (4–6 MPa nitrogen) for leak detection. After confirming no leaks, the nitrogen is released, and the reactor undergoes 3–5 cycles of evacuation and nitrogen refilling before final evacuation. The system is heated to the target temperature and maintained for 24 h. Upon reaction completion, gases are released when the temperature drops to 200 °C. Pyrolysis gases pass through a liquid nitrogen-cooled condensate trap, followed by an ice-water-cooled spiral condenser, and finally into a metering tube for volume measurement and compositional analysis. To prevent light hydrocarbon loss, condensate and water in the trap are separated by adding dichloromethane (DCM), followed by triple DCM extraction. The condensate in DCM is quantified via chromatography and gravimetry. Oil residues adhering to the reactor surfaces are rinsed with DCM, and after DCM evaporation, the expelled light hydrocarbons are collected. This testing was performed by the Organic Geochemistry Laboratory of the Daqing Oilfield Exploration and Development Research Institute, PetroChina.

Fluid inclusions represent portions of formation fluids trapped during diagenetic mineral crystallization. The homogenization temperature method of fluid inclusions provides an accurate means to determine hydrocarbon accumulation timing. The principle relies on the fact that aqueous inclusions in deep reservoirs initially exist as single liquid phase, which separate into gas–liquid biphasic systems upon surface sampling due to temperature–pressure reduction. Experimental evidence confirms temperature as the dominant controlling factor. When heated on a microthermometry stage until gas phase disappearance, the temperature at which complete liquid phase homogenization occurs represents the original formation temperature in deep reservoirs. This temperature, com

bined with the basin's paleogeothermal model and burial history, enables determination of both the formation depth and corresponding geological age of the inclusions, thereby constraining hydrocarbon accumulation timing [35–37]. The homogenization temperatures of fluid inclusions were measured using a THMSG600, DM4500P cold and hot microplatform (Linkam Company, Oxfordshire, UK). The experiment was conducted in the State Key Laboratory of Continental Dynamics, Northwest University, Xi'an, China.

## 4. Results

### *4.1. Determination of Hydrocarbon Accumulation Period Through Source Rock Generation-Expulsion History*

Simulation results of hydrocarbon generation and expulsion history in the Huhu Depression (Table 1) indicate that the source rocks began expelling hydrocarbons at the end of Damoguaihe Formation deposition (approximately 125 Ma), with relatively small expulsion volumes. By the end of Yimin Formation deposition (around 100 Ma), the expulsion area expanded significantly, marking the peak expulsion period. During subsequent geological periods, the expulsion volumes progressively increased. Notably, the expulsion volume during the Yimin Formation period accounted for nearly half of the total expulsion (Figure 2), while the period since Qingyuangang Formation deposition contributed the remaining half.

**Table 1.** Hydrocarbon generation and expulsion volumes in different geological periods in Huhehu sag.

| Horizon | Present-Day | | Top Yimin Fm | | Top Damoguaihe Fm | |
|---|---|---|---|---|---|---|
| | Total Hydrocarbon Generation ($10^8$ t) | Hydrocarbon Expulsion Volume ($10^8$ t) | Total Hydrocarbon Generation ($10^8$ t) | Hydrocarbon Expulsion Volume ($10^8$ t) | Total Hydrocarbon Generation ($10^8$ t) | Hydrocarbon Expulsion Volume ($10^8$ t) |
| $K_1d_2$ | 0.798 | 0 | 0.669 | 0 | 0.229 | 0 |
| $K_1d_1$ | 3.98 | 0.433 | 3.07 | 0 | 1.66 | 0 |
| $K_1n_2$ | 3.91 | 1.8 | 3.41 | 1.43 | 1.25 | 0 |
| $K_1n_1$ | 2.55 | 1.31 | 2.5 | 1.24 | 1.04 | 0.35 |
| Total | 11.2 | 3.55 | 9.65 | 2.67 | 4.19 | 0.35 |

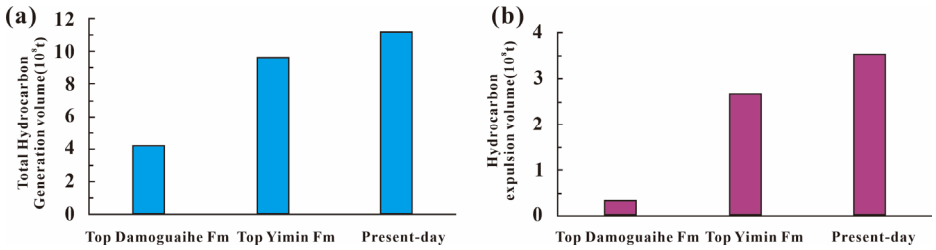



**Figure 2.** Distribution graph of hydrocarbon generation (**a**) and expulsion volumes (**b**) in different geological periods in Huhehu sag.

The hydrocarbon expulsion history reveals two distinct reservoir formation stages: the Yimin Formation depositional period and the period from Qingyuangang Formation deposition to present.

### *4.2. Determination of Hydrocarbon Accumulation Using Authigenic Illite Dating Method*

Authigenic illite in sandstone reservoirs represents the latest diagenetic mineral formed before hydrocarbon charging in potassium-rich aqueous environments, with its formation ceasing upon hydrocarbon emplacement. Consequently, illite dating serves as an effective method for determining hydrocarbon accumulation timing [38,39].

This study used the latest version of the International Chronostratigraphic Chart (2023 edition) published by the International Commission on Stratigraphy (ICS). Twelve hydrocarbon-bearing core samples were collected from producing formations in the

Huhehu, Beier, Wuerxun, and Hulun Lake sags of the Hailar Basin. The selected samples were analyzed by isotope chronology. Dating results yielded excellent consistency, showing illite ages of 92.52–98.74 Ma for oil-bearing reservoirs. These ages are highly consistent with dating results from the basin's major oil-producing sags (Wuerxun, Beier, and Hulun Lake) as shown in Table 2 and Figure 3, indicating hydrocarbon accumulation occurred during the early period of the Qingyuangang Formation deposition. There is a deficiency in that there are only two illite dating samples from Nantun Formation in Huhehu sag. If samples from different strata can be collected in the future, the research effect may be better.

**Table 2.** Results of authigenic illite dating of hydrocarbon reservoirs in Hailar basin.

| Depression | Well Number | Well Depth (m) | Horizon | Age (Ma) |
|---|---|---|---|---|
| Beier Depression | Huo-3 | 2023 | Tongbomiao Formation | 93.73 ± 2.0 |
| | Huo-3 | 2023 | | 98.74 ± 2.0 |
| Wuerxun Depression | Wu-11 | 1895 | | 93.28 ± 2.0 |
| | Wu-11 | 1895 | | 93.07 ± 2.0 |
| | Su-6 | 1520 | Damoguaizi Formation | 94.87 ± 2.0 |
| | Su-6 | 1520 | | 92.52 ± 2.0 |
| Hulun Lake Depression | HS-3 | 2076 | Tongbomiao Formation | 96.71 ± 2.0 |
| | HS-3 | 2076 | | 95.3 ± 2.0 |
| | HS-3 | 1526 | Nantun Formation | 92.71 ± 2.0 |
| | HS-3 | 1526 | | 94.5 ± 2.0 |
| Huhehu Depression | He-2 | 1646 | | 96.67 ± 2.0 |
| | He-2 | 1646 | | 96.14 ± 2.0 |

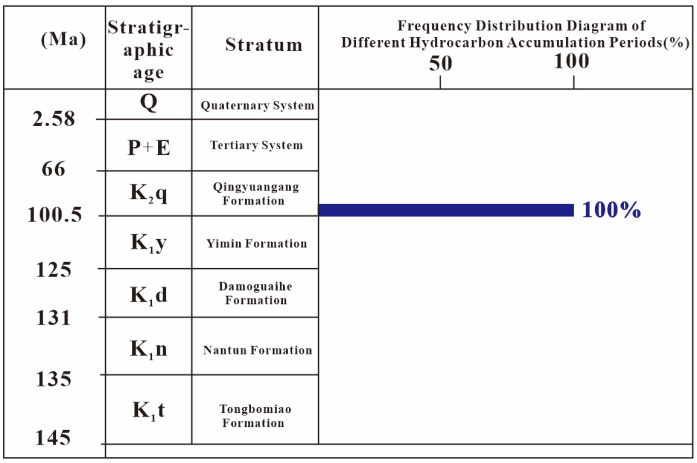



**Figure 3.** Frequency distribution of oil-gas reservoirs formation stages of illite dating in Huhehu sag.

### *4.3. Determination of Hydrocarbon Accumulation Period Using Homogenization Temperatures of Reservoir Fluid*

It is very important to judge the formation period of oil and gas reservoirs by using the homogenization temperature method of inclusions and accurately restore the burial history and thermal evolution history of the basin, especially the thermal evolution history of the basin, and even directly judge the formation period of oil and gas reservoirs [40–44]. The Huhehu Sag experienced significant uplift and erosion after the Yimin Formation deposition, where the relationship between eroded thickness and subsequent re-deposition critically influences accumulation timing determinations. Vitrinite reflectance (Ro) versus current burial depth (H) analysis identifies the Huhehu Sag as an uplift-erosion type depression currently in an undercompensated state (Figure 4). Thermal history simulation is based on important constraints such as geological thickness, geological age, and erosion

thickness during critical periods. Combined with geothermal field parameters and measured vitrinite reflectance values, the thermal history of Well He 1 was simulated by the PetroMod(2016) developed by Schlumberger, Houston, TX, USA [45,46].

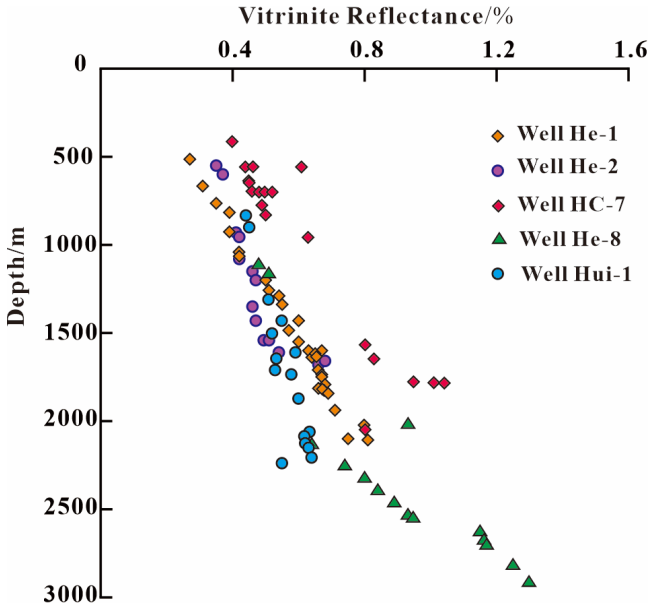



**Figure 4.** Relation graph between vitrinite reflectance and depth in Huhehu sag.

Three oil-bearing sandstone samples with well-developed inclusions from the Huhehu Sag were selected for microthermometric analysis. The inclusions predominantly occur along quartz microfractures, in quartz veins, and within calcite cement, exhibiting linear distribution patterns. Microscopically colorless to pale yellow, they display elliptical, triangular, and irregular shapes with gas–liquid ratios ranging from 0.5% to 15%. Homogenization temperatures range from 88 to 175 °C (Table 3).

**Table 3.** The fluid inclusion homogenization temperature in Huhehu sag.

| Well | Depth (m) | Horizon | Lithology | Homogenization Temperature (°C) |
|---|---|---|---|---|
| He-1-1 | 1634.81~1641.18 | First Member of Damoguaihe Formation | Oil-bearing fine sandstone | 90, 92, 93, 94, 98, 155, 156, 157, 160, 163, 165, 170 |
| He-1-2 | 1845.13~1853.7 | Second Member of Nantun Formation | Sandstone | 88, 90, 92, 94, 95, 96, 98, 155, 157, 159, 160, 165, 167, 170 |
| He-2 | 1637.24~1655.1 | Second Member of Nantun Formation | Oil-impregnated coarse sandstone | 92, 96, 91, 99, 98, 100, 158, 159, 164, 166, 167, 170, 171, 175 |

Analysis of homogenization temperatures from fluid inclusions in the Second Member of Nantun Formation (Well He-1 and Well He-2, Huhu Depression) reveals two distinct ranges: 88–100 °C and 155–175 °C (Figure 5). According to the thermal evolution history from Well He-1, these data indicate paleotemperatures never exceeded 150 °C since Nantun Formation deposition, suggesting the higher temperature range (155–175 °C) reflects deep-sourced fluids. The 88–100 °C homogenization temperatures constrain hydrocarbon accumulation in Nantun Formation sandstones to 126–87 Ma (Yimin Formation depositional period, Figure 6).

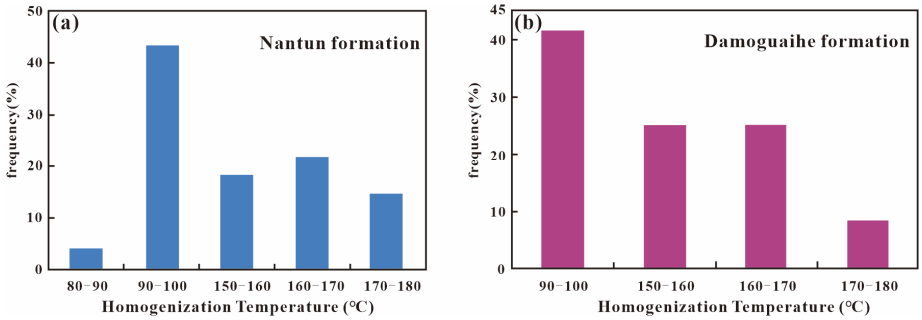



**Figure 5.** Histogram of the fluid inclusion homogenization temperature in Huhehu sag. (**a**) Nantun formation; (**b**) Damoguaihe formation.

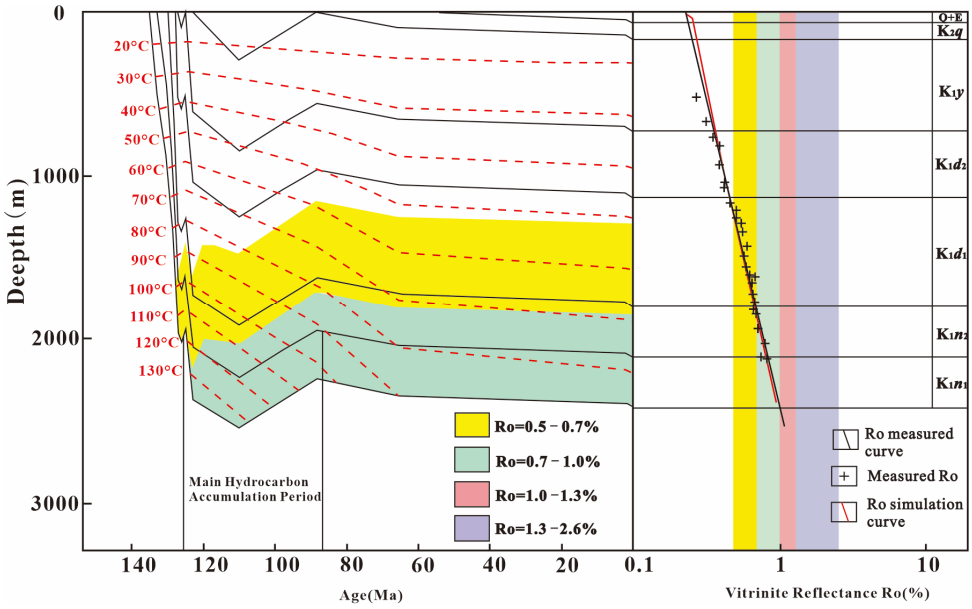



**Figure 6.** Thermal history of He1 and hydrocarbon accumulation period in Huhehu sag.

## 5. Discussion

From the perspective of geological evolution in the Huhehu Sag, hydrocarbon accumulation is closely correlated with tectonic development history. During the Early Cretaceous, the Hailar Basin underwent rift development with generally high geothermal gradients. The Nantun Formation depositional period represented the primary subsidence phase, featuring the following: (1) Lacustrine source rock development; (2) maximum sedimentation rates reaching 420 m/Ma in depression centers; (3) elevated geothermal gradients of 41–49 °C/km (Figure 7) [47]. The Damoguaihe Formation period witnessed stable extensional rifting characterized by the following: (1) rapid, large-scale subsidence (up to 780 m/Ma sedimentation rates); (2) intense volcanic activity creating volcanism-induced high thermal regimes (50–55 °C/km) [47]; and (3) accelerated thermal maturation of source rocks into the main hydrocarbon generation window. During deposition of the Second and Third Members of Yimin Formation, the following occurred: (1) large-scale traps became structurally configured; (2) the Tongbomiao and Nantun source rocks reached peak expulsion during Yimin Formation deposition; (3) partial Damoguaihe source rocks entered the expulsion peak; and (4) pre-Yimin Formation trap formation ensured optimal timing for hydrocarbon capture. Thermal modeling confirms this period as (1) the primary accumulation phase [47,48]; (2) the maximum paleotemperature interval [13]; and (3) coinciding with regional lithospheric thinning and volcanic climax in Northeast China [49].

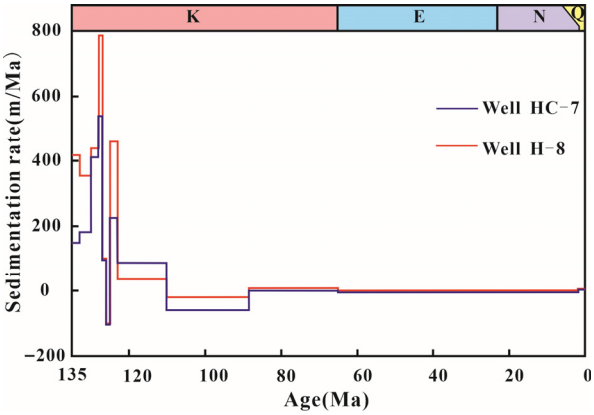



**Figure 7.** Sedimentary rate evolution history of the Huhehu sag (K-Cretaceous, E-Paleogene, N-Neogene, Q-Quaternary).

During the late Early Cretaceous, the basin underwent structural inversion under NW–SE compressional stress, resulting in uplift of the Hailar Basin and regional strata erosion. This tectonic activity led to decreased formation temperatures and a gradual reduction in the geothermal gradient to the current 35.4 °C/km, consequently further weakening hydrocarbon generation in source rocks [50]. Since the Late Cretaceous, the Huhehu Sag has entered a depression development stage characterized by lake basin shrinkage and diminished subsidence rates. While hydrocarbon reservoirs experienced readjustment, the central depression maintained elevated formation temperatures up to 110 °C due to deep burial by overlying strata. The Nantun Formation source rocks continued hydrocarbon expulsion, with secondary generated hydrocarbons migrating upward to accumulate in traps (Figure 8). Currently, discovered hydrocarbons predominantly originate from the Nantun Formation, with minor contributions from Member 1 of the Damoguaihe Formation [22,23].

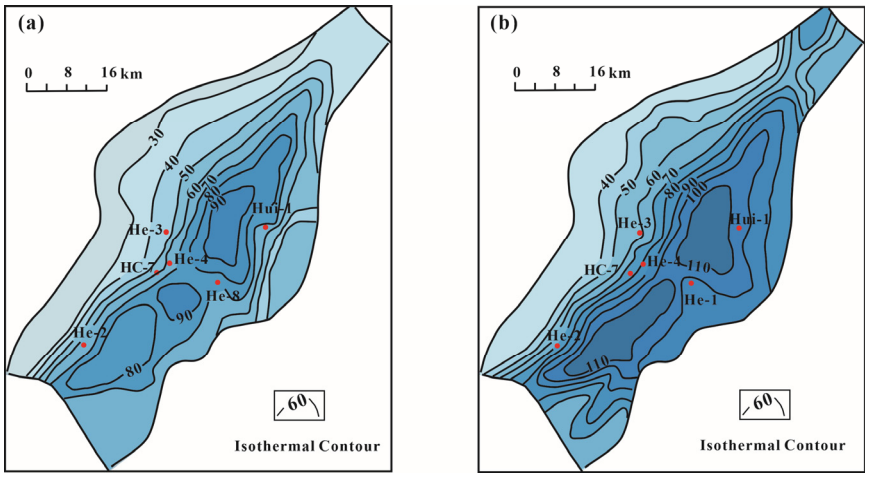



**Figure 8.** Plane map showing distribution of present temperature in Huhehu sag. (**a**) Nantun formation; (**b**) Damoguaihe formation.

Analysis of discovered reservoirs indicates that fault-block reservoirs and fault-lithologic reservoirs represent the predominant types, typically exhibiting zonal distribution along both gentle and steep slopes of the sag. Lithologic reservoirs are primarily distributed within or near source kitchens, showing relatively limited spatial extent (Figure 9). As a typical half-graben rift basin with rapid sedimentary facies changes, the Huhehu Sag is characterized by predominantly short-distance hydrocarbon migration. Consequently, structural zones beyond source kitchens rarely develop enriched reservoirs. The most

favorable hydrocarbon accumulation zones are located in and around source kitchens where reservoirs with favorable physical properties are developed.

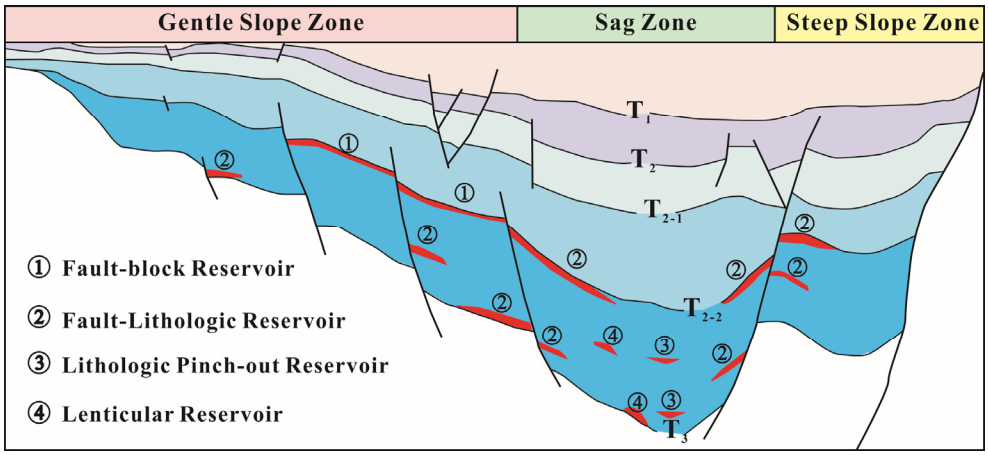



**Figure 9.** The accumulation model schematic graph of oil and gas in Huhehu sag.

## 6. Conclusions

Integrated analysis using multiple methods indicates two principal hydrocarbon accumulation phases in the Huhehu Sag. The first phase (approximately 90–125 Ma), during the Yimin Formation depositional period, represents the paleothermal maximum and primary hydrocarbon accumulation epoch. During this critical interval, source rocks underwent extensive hydrocarbon generation and expulsion, with sufficient hydrodynamic pressure and buoyancy forces facilitating effective hydrocarbon transport and trap filling. The second phase extends from the Qingyuangang Formation deposition to the present day. The Yanshanian orogeny at the Yimin Formation's depositional terminus caused basin-wide uplift and erosion in the Hailar Basin, reducing formation temperatures and diminishing source rock hydrocarbon generation, thereby triggering the modification and redistribution of primary hydrocarbon accumulations.

As a characteristic half-graben rift basin, the Huhehu Sag is predominantly characterized by fault-block and fault-lithologic reservoirs, typically distributed in belts along both gentle and steep slopes. Lithologic reservoirs are principally confined to central and proximal areas of source kitchens. The most favorable hydrocarbon accumulation zones occur in central source kitchen areas and adjacent regions with well-developed reservoirs featuring favorable petrophysical properties.

**Author Contributions:** Writing—original draft preparation, writing—review and editing, investigation, J.C.; formal analysis, W.J.; resources and investigation, Z.R.; data analysis and map editing, H.S.; software and translation, G.L.; data curation, H.T. All authors have read and agreed to the published version of the manuscript.

**Funding:** This study was supported by the General Program of the National Natural Science Foundation of China (Nos. 41772121, 41002040).

**Data Availability Statement:** The data used to support the findings of this study are available from the first author upon request (first author: cuijp@nwu.edu.cn).

**Conflicts of Interest:** Author Wei Jin was employed by the company Exploration and Development Research Institute, Daqing Oilfield, China National Petroleum Corporation. The remaining authors declare that the research was conducted in the absence of any commercial or financial relationships that could be construed as a potential conflict of interest.

## References


1. Hao, F.; Zou, H.Y.; Jiang, J.Q. Dynamics of petroleum accumulation and its advances. *Earth Sci. Front.* **2000**, *7*, 11–22.
2. Xin, R.C.; Tian, C.Z.; Dou, T.J. Study of oil-pool-forming chronology. *Earth Sci. Front.* **2000**, *7*, 48–54.
3. Jiang, Z.X.; Pang, X.Q.; Huang, Z.L. A method for studying the oil and gas migration stages in superposed basin and its application. *Oil Explor. Dev.* **2000**, *27*, 22–25.
4. Ren, Z.L.; Cui, J.P.; Feng, J.H.; Ren, L.Y.; Liu, L. Research on formation stages of hydrocarbon reservoirs in Qiaokou area of Dongpu depression. *Oil Explor. Dev.* **2002**, *29*, 15–18.
5. Ren, Z.L.; Feng, J.H.; Cui, J.P.; Ren, L.Y. Formation stages of natural gas reservoirs in Duqiaobai area of Dongpu depression. *Oil Gas Geol.* **2002**, *23*, 376–381.
6. Zhao, M.J.; Song, Y.; Pan, W.Q.; Han, J.F.; Liu, S.B.; Qin, S.F. The overall approach of hydrocarbon filling periods and process in sedimentary basins. *Adv. Earth Sci.* **2004**, *19*, 939–946.
7. Liu, G.D.; Zhang, Z.P.; Chen, W.X.; Chen, W.L.; Lin, S.Q. Study on the period and time of oil and gas accumulation in Yanqi basin, Northwest China. *Oil Explor. Dev.* **2002**, *29*, 69–71.
8. Xiao, H.; Ren, Z.L.; Cui, J.P. Studies of accumulation stages of Silurian gas-bearing reservoirs in well Kongqu 1 in the Tarim basin. *Pet. Geol. Exp.* **2008**, *30*, 357–362.
9. Suggate, R.P. Relations between depth of burial, vitrinite reflectance and geothermal gradient. *J. Pet. Geol.* **1998**, *21*, 5–32. [CrossRef]
10. Sweeney, J.J.; Burnham, A.K. Evaluation of a simple model of vitrinite reflectance based on chemical kinetics. *AAPG Bull.* **1990**, *74*, 1559–1570. [CrossRef]
11. Gallagher, K. Evolving temperature histories from apatite fission-track data. *Earth Planet. Sci. Lett.* **1995**, *136*, 421–435. [CrossRef]
12. Muirhead, D.K.; Bond, C.E.; Watkins, H.; Butler, R.W.H.; Schito, A.; Crawford, Z.; Marpino, A. Raman Spectroscopy: An effective thermal marker in low temperature carbonaceous fold-thrust belts. *Geol. Soc. Lond. Spec. Publ.* **2019**, *490*, 135–151. [CrossRef]
13. Sanità, E.; Di Rosa, M.; Lardeaux, J.M.; Marroni, M.; Tamponi, M.; Lezzerini, M.; Pandolfi, L. Deciphering the pressure–temperature path in low-grade metamorphic rocks by combining crystal chemistry, thermobarometry and thermodynamic modelling: An example in the Marguareis Massif, Western Ligurian Alps, Italy. *Miner. Mag.* **2025**, *89*, 203–224. [CrossRef]
14. Ren, Z.L.; Qi, K.; Yang, G.L.; Cui, J.P.; Yang, P.; Wang, K. Research status and existing problems of relationship between deep thermal evolution history and oil and gas in sedimentary basins. *Unconv. Oil Gas.* **2020**, *7*, 1–7.
15. Zhang, X.D.; Liu, G.D.; Wang, J.L. Structural Characters of the Hailar Basin and Its Geological Evolution. *Pet. Geol. Exp.* **1994**, *16*, 119–127.
16. Zhang, Y.Q.; Zhao, Y.; Dong, S.W.; Yang, N. Tectonic evolution stages of the Early Cretaceous rift basins in Eastern China and adjacent areas and their geodynamic background. *Earth Sci. Front.* **2004**, *11*, 123–133.
17. Lu, S.F.; Liu, X.Y.; Qu, J.Y.; Wang, Z.W. Restoring of Original Hydrocarbon Potential and Original Organic Carbon of Source Rocks in Huhehu Depression of Hailar Basin. *J. Northeast Pet. Univ.* **1995**, *19*, 31–34.
18. Lu, S.F.; Wang, Z.W.; Chen, X. Application of Kinetic Method on Hydrocarbon Generation to Evaluation Source Rocks in Huhehu Depression. *Explorationist* **1997**, *2*, 41–46.
19. Cui, J.P.; Ren, Z.L.; Xiao, H. Relations between the Thermal History and Petroleum Generation in the Huhehu Depression, Hailar basin. *Geol. China.* **2007**, *34*, 522–527.
20. Wang, P.J.; Zhong, J.H.; Niu, Y.B. Tectonic Feature and Evolution of Huhehu Depression in Hailar Basin. *Spec. Oil Gas Reserv.* **2009**, *16*, 25–27.
21. Liu, H.Y. The Evalution of Hydrocarbon Source Rock in Huhehu Depression. Master's Thesis, Northeast Petroleum University, Daqing, China, 2010; pp. 8–34.
22. Lu, K.; Hou, D.J.; Hong, H.F.; Cao, H.M. Geochemical Characteristics of Crude Oil and Correlation of Oil Source in Huhehu Sag. *J. Guilin Univ. Technol.* **2010**, *30*, 28–32.
23. Shen, W.J. Geochemical Characteristics and the Origin of Gas from He 10 Well, Huhehu Depression in Hailar Basin. *Nat. Gas Explor. Dev.* **2010**, *33*, 22–26.
24. Li, J.H.; Lu, S.F.; Meng, Q.A.; Cao, R.C.; Zhu, D.F.; Liu, H. Tectonic Evolution and Its Controlling on Hydrocarbon of Huhehu Depression in Hailar Basin. *Chin. J. Geol.* **2011**, *46*, 929–941.
25. Wu, C.B.; Li, J.H. Sequence Stratigraphic Geochemistry and Its Application to the Evaluation of Source Rocks of Huhehu Sag in Hailar Basin. *Acta Geol. Sin.* **2012**, *86*, 661–670.
26. Liu, S.G.; Luo, Z.L.; Zhao, X.K.; Long, X.M.; Wang, D.N.; Zhang, E.H.; Li, A.F. Studying the Evolution of the Hailaer Basin, NeiMengGu. *J. Chengdu Coll. Geol.* **1993**, *20*, 78–86.
27. Chen, J.L.; Wu, H.Y.; Zhu, D.F.; Lin, C.H.; Yu, D.S. Tectonic Evolution of the Hailar Basin and Its Potentials of Oil-gas Exploration. *Chin. J. Geol.* **2007**, *42*, 147–159.

28. Sanità, E.; Conconi, R.; Lorenzon, S.; Di Rosa, M.; Capitani, G.; Mugnaioli, E. Application of an improved TEM-EDS protocol based on charge balance for accurate chemical analysis of sub-micrometric phyllosilicates in low-grade metamorphic rocks. *Clays Clay Miner.* **2024**, *72*, 1–11. [CrossRef]
29. Hamilton, P.J.; Kelley, S.; Fallick, A.E. K-Ar dating of illite in hydrocarbon reservoirs. *Clay Miner.* **1989**, *24*, 215–231. [CrossRef]
30. Wang, F.Y.; Hao, S.S.; Lei, J.J. The isotopic dating of authigenic illite and timing of hydrocarbon fluid emplacement in sandstone reservoir. *Acta Pet. Sin.* **1998**, *19*, 40–43.
31. Zhang, Y.Y.; Luo, X.Q.; Song, J. Discussions on K-Ar isotopic geochronological studies of authigenic illites in hydrocarbon reservoirs. *Geoscience* **2002**, *16*, 403–407.
32. Hunt, J.M.; Lewan, M.D. Modeling oil generation with time-temperature index graphs based on the Arrhenius equation. *AAPG Bull.* **1991**, *75*, 795–807. [CrossRef]
33. Xu, S.H.; He, S.; Yuan, C.P. A simulation model of histories of evolution and hydrocarbons generation and expulsion of source rock. *Earth Sci.-J. China Univ. Geosci.* **1995**, *20*, 335–341.
34. He, C.; Zhang, L.J.; Wang, Q.; Ma, Z.L.; Ma, J.F. Experiment development and application of source rock thermal simulation for hydrocarbon generation and expulsion. *Pet. Geol. Exp.* **2021**, *43*, 862–870.
35. Wang, H.J.; Cai, Y.C. Applications of general characteristics of fluid inclusions to the study of oil and gas pool formation. *Oil Explor. Dev.* **2000**, *27*, 50–52.
36. Liu, S.B.; Gu, J.Y. Analytical methods of fluid inclusions and applications to the study of oil and gas. *Oil Explor. Dev.* **1997**, *24*, 29–33.
37. Zhang, M.J.; Tang, J.H.; Zhang, T.W.; Lv, Z.G.; Yang, R.S. Applications of Fluid Inclusions to Petroleum and Natural Gas Geology and Geochemistry. *Geol. Rev.* **2004**, *50*, 397–406.
38. Liewig, N.; Clauer, N.; Sommer, F. Rb-Sr and K-Ar Dating of Clay Diagenesis in Jurassic Sandstone Oil Reservoir, North Sea1. *AAPG Bull.* **1987**, *71*, 1467–1474.
39. Wang, F.Y.; He, P.; Zhang, S.C.; Zhao, M.J.; Lei, J.J. The K-Ar isotopic dating of authigenic illites and timing of Hydrocarbon fluid emplacement in sandstone reservoir. *Geol. Rev.* **1997**, *43*, 541–545.
40. Ren, Z.L.; Liu, L.; Cui, J.P.; Xiao, H.; Gao, S.L. Application of tectoni-thermal evolution history to hydrocarbon accumulation timing in sedimentary basins. *Oil Gas Geol.* **2008**, *29*, 502–506.
41. Ren, Z.L. Research on the relations between geothermal history and oil-gas accumulation in the Ordos basin. *Acta Pet. Sin.* **1996**, *17*, 17–24.
42. Ren, Z.L.; Liu, C.Y.; Zhang, X.H.; Wu, H.N. Research on the relations between geothermal history and oil-gas generation in Jiudong basin. *Acta Sedimentol. Sin.* **2000**, *18*, 619–623.
43. Qiu, N.S. Thermal evaluation and hydrocarbon generation history of the sedimentary basins in western China. *Oil Explor. Dev.* **2002**, *29*, 6–8.
44. Ren, Z.L.; Liu, C.Y.; Pu, R.H.; Li, J.B.; Feng, J.H. Research on geothermal history of Bayindoulan depression in Erlian basin. *Acta Pet. Sin.* **2000**, *21*, 42–45.
45. Sykes, R.; Snowdon, L.R. Guidelines for assessing the petroleum potential of coaly source rocks using Rock-Eval pyrolysis. *Org. Geochem.* **2002**, *33*, 1441–1455. [CrossRef]
46. Opera, A.; Alizadeh, B.; Sarafdokht, H.; Janbaz, M.; Fouladvand, R.; Heidarifard, M.H. Burial history reconstruction and thermal maturity modeling for the middle cretaceous–Early miocene petroleum System, southern Dezful Embayment, SW Iran. *Int. J. Coal Geol.* **2013**, *120*, 1–14. [CrossRef]
47. Cui, J.P.; Zhao, J.; Ren, Z.L.; Jin, W.; Xing, L.; Wang, Y.Q. Geochemical Characteristics of Lower Cretaceous Source Rocks and Thermal History in the Huhehu Depression, Hailar Basin. *Earth Sci.* **2020**, *45*, 238–250.
48. Dong, L.; Wang, W.M.; Yu, X.B.; Wang, G.H. Study on Hydrocarbon Accumulation Stages in Nantun Formation, Huhehu Depression, Hailaer Basin. *Pet. Geol. Recovery Effic.* **2011**, *18*, 20–23.
49. Zhou, J.B.; Zhang, X.Z.; Ma, Z.H.; Liu, L.; Jin, W.; Zhang, M.S.; Wang, C.W.; Chi, X.G. Tectonic Frame Work and Basin Evolution in Northeast China. *Oil Gas Geol.* **2009**, *30*, 530–538.
50. Zhang, X.Z.; Guo, Y.; Zeng, Z.; Fu, Q.L.; Pu, J.B. Dynamia Evolution of the Mesozoic-Cenozoic Basins in the Northeastern China. *Earth Sci. Front.* **2015**, *22*, 88–98.


**Disclaimer/Publisher's Note:** The statements, opinions and data contained in all publications are solely those of the individual author(s) and contributor(s) and not of MDPI and/or the editor(s). MDPI and/or the editor(s) disclaim responsibility for any injury to people or property resulting from any ideas, methods, instructions or products referred to in the content.